

SCIENTIFIC REPORTS



OPEN

Selection preserves Ubiquitin Specific Protease 4 alternative exon skipping in therian mammals

Caitlyn Vlasschaert^{1,3,4}, Xuhua Xia^{2,3} & Douglas A. Gray^{1,4}

Received: 02 September 2015

Accepted: 23 December 2015

Published: 02 February 2016

Ubiquitin specific protease 4 (USP4) is a highly networked deubiquitinating enzyme with reported roles in cancer, innate immunity and RNA splicing. In mammals it has two dominant isoforms arising from inclusion or skipping of exon 7 (E_7). We evaluated two plausible mechanisms for the generation of these isoforms: (A) E_7 skipping due to a long upstream intron and (B) E_7 skipping due to inefficient 5' splice sites (5'SS) and/or branchpoint sites (BPS). We then assessed whether E_7 alternative splicing is maintained by selective pressure or arose from genetic drift. Both transcript variants were generated from a USP4- E_7 minigene construct with short flanking introns, an observation consistent with the second mechanism whereby differential splice signal strengths are the basis of E_7 skipping. Optimization of the downstream 5'SS eliminated E_7 skipping. Experimental validation of the correlation between 5'SS identity and exon skipping in vertebrates pinpointed the +6 site as the key splicing determinant. Therian mammals invariably display a 5'SS configuration favouring alternative splicing and the resulting isoforms have distinct subcellular localizations. We conclude that alternative splicing of mammalian USP4 is under selective maintenance and that long and short USP4 isoforms may target substrates in various cellular compartments.

Ubiquitin-specific protease 4 (USP4) is a deubiquitinating enzyme that can edit or remove ubiquitin chains of various topologies. USP4 can remove both degradative K48- and regulatory K63-linked ubiquitin chains from a growing list of protein targets that include key players in a number of signal transduction pathways. Its substrates include the transforming growth factor- β (TGF- β) I receptor^{1,2} and the TGF- β -activated kinase 1 (TAK1)³, Wnt/ β -catenin pathway transcription factor Nemo-like kinase (NLK)⁴, the p53 antagonist ARF-BP1⁵, anti-viral response mediator RIG-I⁶, TNF α /NF- κ B inflammatory pathway mediators TRAF-2 & -6^{7,8}, and the master growth factor signalling kinase PDK1⁹. Homeostatic regulation of USP4 deubiquitination targets is provided by the opposing actions of E3 ubiquitin ligase enzymes that promote degradation or complex assembly.

USP4 has both nuclear importing and exporting signal motifs and can shuttle between nucleus and cytoplasm¹⁰. Subcellular localization is partially controlled by AKT-mediated phosphorylation of the serine residue at position 445, which promotes cytoplasmic retention². Nuclear localization, coupled with the observation that USP4 interacts with at least eleven splicing factors¹¹ including Prp3¹², suggests that USP4 regulates spliceosomal activity. This is particularly interesting since multiple spliced variants of USP4 have been reported in human. The two major isoforms differ by the inclusion of Exon 7 (E_7 ; Fig. 1), though neither differential activities nor specificities have been attributed to the resulting long and short isoforms since their discovery^{13,14} shortly after that of the gene itself¹⁵. The two isoforms (with or without E_7) both produce functional USP4 proteins in deubiquitination assays¹⁴. E_7 forms the major part of the flexible linker region that enables the critical interaction of the neighbouring DUSP-UBL1 and insert domains of USP4 (Fig. 1B). In the E_7 -skipped (short) isoform, the linker is shortened from sixty-seven to twenty amino acids though retains sufficient flexibility to enable comparable domain interaction¹⁶. Despite the proposed facultative role of this alternatively spliced exon¹⁶, the majority of conserved phosphorylation sites in USP4 are within E_7 , suggesting the protein isoforms may be differently regulated¹⁷. What is more, the longer variant is the principal isoform and the relative amount of exon-skipped transcripts is consistent within but different among tissue types, suggesting alternative splicing may be regulated¹⁴. The mechanism for E_7 skipping in human USP4 mRNA is not known, nor are the functional implications of this alternative splicing.

¹Ottawa Hospital Research Institute, Ottawa, K1H 8L6, Canada. ²Department of Biology, University of Ottawa, Ottawa, K1N 6N5, Canada. ³Ottawa Institute of Systems Biology, Ottawa, K1H 8M5, Canada. ⁴Department of Biochemistry, Microbiology and Immunology, University of Ottawa, Ottawa, K1H 8M5, Canada. Correspondence and requests for materials should be addressed to X.X. (email: xxia@uottawa.ca) or D.A.G. (email: dgray@ohri.ca)

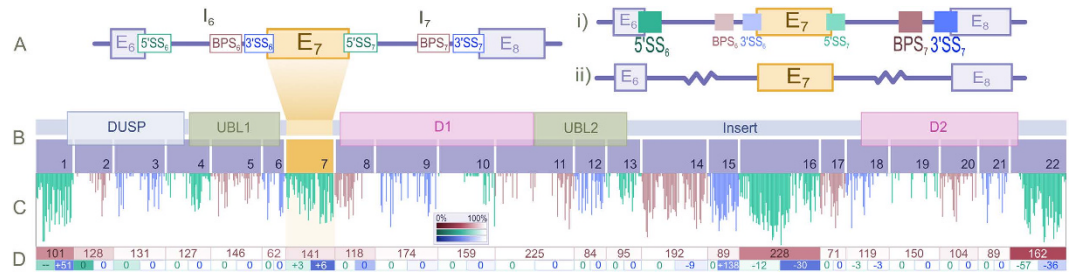


Figure 1. Schema of *Usp4* exonic properties and potential mechanisms of exon skipping. (A) Proposed alternative mechanisms for skipping of exon 7 in USP4: (i) differential splice site strengths (ii) long flanking introns (B) *Usp4* exon structure relative to encoded protein domains. *D1* and *D2* form the cysteine protease catalytic domain that effectuates ubiquitin cleavage. The regulatory *DUSP-UBL1* domain physically interacts with the unstructured *Insert* region and with *DUSP-UBL1* domains of other USP4 monomers leading to dimerization. (C) USP4 protein sequence entropy. USP4 exon-retained isoform amino acid sequences for 62 species were aligned using MUSCLE⁵¹. Shannon entropy was calculated using DAMBE⁵⁰ and plotted using the ggplot2⁵² package in R. (D) Exon length variability. Mode of length per exon (in nucleotides) for 37 mammals indicated in pink boxes. Mode of 33 birds and 24 fish exon lengths relative to mammalian mode (codon indels) indicated in green and blue boxes, respectively. Shading of boxes indicates fraction of total sequences represented by the mode, where darkening is commensurate with increasing variability (see inset legend above).

Exon skipping is the most frequent form of alternative splicing and accounts for about 40% of all alternative splicing in higher eukaryotes^{18–20}. A number of exon skipping mechanisms have been proposed, including:

1. differential strength of splice signals leading to alternative splice site selection (reviewed in Keren *et al.*²¹).
2. excessively long flanking introns^{22–27}.
3. intermixture of major and minor class introns²⁸.

As USP4 does not have minor class introns, we chose to examine the first two mechanisms of *E*₇ skipping, as illustrated in Fig. 1A(i,ii). First, if an exon is functionally important, then flanking sequences recognized by splicing factors will be under strong purifying selection to maintain proper spliced end-products. If the inclusion of *E*₇ is unimportant, then its proximal splice sites (3'SS₆, 5'SS₇, and BPS₆) may experience greater sequence drift, leading to weakening of these sites relative to 5'SS₆, 3'SS₇ and BPS₇ and exon 7 skipping (Fig. 1A(i)). Selection can however also act to preserve differential splice signal strengths in order to enable the production of two isoforms. In short, strong 5'SS₆, 3'SS₇ and BPS₇ relative to 5'SS₇, 3'SS₆ and BPS₆, resulting from passive drift or active selection, could permit *E*₇ skipping. Second, exons flanked by long introns are known to be intermittently skipped. As such, the alternative inclusion of *E*₇ in USP4 mRNA could be explained by appropriately long flanking introns (Fig. 1A(ii)). We evaluated these alternative hypotheses by constructing a computational evolutionary framework to characterize USP4 splicing patterns in multiple vertebrate lineages and tested our *in silico* predictions in the laboratory to gauge whether the two isoforms of USP4 observed in humans have discrete functional and/or regulatory roles or whether they are the by-product of reduced selection for *E*₇ retention.

Results

Bioinformatic analysis. To study exon-intron architecture and splice signal conservation, we downloaded GenBank sequences for well-annotated USP4 sequences for 62 vertebrate species covering major vertebrate taxa (see Supplementary Table S1).

Sequence and length conservation of USP4 exons. Both long and short isoforms of USP4 comprise a bi-partite catalytic domain and a regulatory DUSP-UBL1 domain, where the seventh exon forms part of the unstructured flexible linker between these two (Fig. 1B). Sequence identity (Fig. 1C) and length (Fig. 1D) of USP4 exons are highly conserved for exons that encode structured functional domains and less well for exons that correspond to unstructured regions. *E*₇ exhibits greater length variation than its neighbors. Relative to mammals, *E*₇ of birds and fish generally encodes one and two additional amino acids respectively, while the length of *E*₇ within each of these clades is variable; this suggests multiple indel events in USP4 during the evolutionary diversification of vertebrates. Sequence conservation among aligned USP4 exons, quantified using Shannon entropy in Fig. 1C, reveals that *E*₇ is located within a highly variable region. The entropic nature of *E*₇ conforms to the general pattern that alternatively spliced exons exhibit less sequence conservation²⁹, which can extend to exon-intron boundaries and thus weaken the signals of proximal splice sites. However, high entropy is also observed in all other USP4 exons coding for unstructured regions (i.e., exons 1, 14, 15, 16, 17, 22), which are not alternatively spliced. The disordered nature of the unstructured region encoded by *E*₇ could simply permit its sequence variability and the splice sites may not be affected. To determine whether *E*₇ neighboring splice site signals are weakened, we quantified their strengths relative to the optimal sequences recognized by the spliceosome.

Relative strengths of branchpoint site signals. The signal strength of a branch point site (BPS) in vertebrates is generally contingent upon the presence of a YURAY motif located at an optimal distance from 3' end of the intron ($D_{to3'.opt}$) followed by a pyrimidine-rich tract and the AG dinucleotide of the 3'SS signal. $D_{to3'.opt}$ can be



Figure 2. Characterization of relative BPS strengths. (A) Distribution of location of strong BPS sequences (“YURAY” motif with single downstream AG dinucleotide corresponding to the 3’SS) in all introns of human chromosome 22. The X-axis depicts the last 200 nt of the introns. Introns shorter than 200 nt were excluded to avoid statistical bias. $D_{to3',opt}$ is 20–40 nt. (B) Locations of YURAY sequences within 50nt of 3’ ends of introns 6 and 7 of USP4 in 14 vertebrate species.

revealed by mapping the intronic locations of several BPS motifs and deriving an optimal range of values for these. A previous analysis of 397 human housekeeping genes reported $D_{to3',opt}$ to be 21–34 nt, representing 83% of introns in these highly expressed genes³⁰. In Fig. 2A, we have derived a more sensitive $D_{to3',opt}$ of 20–40 nt based on the locations of consensus BPS sequences (YURAY) within all 15770 introns of human chromosome 22 protein-coding genes. This slightly larger window for $D_{to3',opt}$ will reduce the false negative rate in detecting true BPSs in the neighbouring introns of E_7 . If a strong BPS is absent from the upstream intron (I_6), a strong downstream BPS within I_7 could lead to exon skipping (Fig. 1A). We therefore evaluated the relative strengths of USP4 BPS₆ and BPS₇ for 14 well-studied species representing the major vertebrate taxa.

The location of YURAY motifs in I_7 (Fig. 2B) suggests a strong BPS₇ among all studied mammalian species. A strong BPS₇ is also present in I_7 of zebrafish (*Danio rerio*), but is missing in the frog (*Xenopus tropicalis*), the chicken (*Gallus gallus*), and the Chinese turtle (*Pelodiscus sinensis*). The latter two species retain candidate YURAY motifs which can be eliminated from consideration due to their greater distance from the 3’SS (73nt for the chicken, 85 nt for the Chinese turtle) and to the presence of a downstream non-3’SS AG (non-3’SS AG dinucleotides between a BPS and a 3’SS AG are avoided as the first AG following the branch-point is generally used as the 3’SS AG).

YURAY motifs are absent from the 40 last nucleotides of USP4- I_6 in all mammalian species. Taken together, mammalian species in general have a weak BPS₆ and a relatively strong BPS₇. This lends plausibility to the first hypothesis from Fig. 1A, wherein E_7 splicing results from alternative pairing of 5’SS₆ and BPS₆ (E_7 skipping) or of 5’SS₇ and BPS₇ (E_7 inclusion). In contrast, non-mammalian species tend to have a strong BPS₆ (except for the Chinese turtle). YURAY motifs are located near $D_{to3',opt}$ in I_6 of the chicken ($D_{to3'} = 47$ nt) and zebrafish ($D_{to3'} = 16$ nt) and frog (three YURAY motifs with $D_{to3'} = 36, 42$ and 53 nt, respectively). This suggests that E_7 skipping should be less likely in non-mammalian than in mammalian species, though the Chinese turtle may be an exception.

Relative strengths of proximal and distal splice signals. In addition to a weak BPS₆ relative to BPS₇, a stronger 5’SS₆ than 5’SS₇ and/or stronger 3’SS₇ than 3’SS₆ would favor E_7 skipping (Fig. 1A(i)). Position weight matrices (PWM) measures site-specific nucleotide usage bias in a motif alignment, where the consensus motif typically has the highest PWM score (PWMS). PWMSs are routinely used to characterize the signal strength of splice sites^{31,32}.

A PWM for the 5’SS sequences of human chromosome 22 introns (Table 1) shows a consensus 5’SS consistent with what has been documented in the literature, i.e., a core motif of AG|GUAAGU, where “|” indicates the exon-intron junction. PWMSs derived from zebrafish and chicken chromosomes are almost identical to the human 5’SS matrix in Table 1 (upper panel). Thus, this PWM can be used to generate PWMSs as comparable measures of signal strength at 5’SS₆ and 5’SS₇ from the 14 representative vertebrate USP4 sequences, where significantly larger scores indicate stronger splice signal strength. Given Table 1 (upper panel), the maximal PWMS is 16.9. PWMSs are consistently larger for 5’SS₆ than 5’SS₇ for the ten mammalian USP4 sequences (Table 1 (lower panel)), with the mean PWMS being 9.2314 for 5’SS₆ and 5.455 for 5’SS₇ ($t = 19.759$, $df = 11$, $p < 0.0001$, paired-sample t-test). This lends support for the scenario depicted in Fig. 1A(i), where a stronger 5’SS₆ favors E_7 skipping in mammals. In contrast, for chicken and zebrafish, PWMS₆ is greater than PWMS₇ while *Pelodiscus sinensis* again conforms to the mammalian pattern (PWMS₆ > PWMS₇).

There were no significant differences in flanking 3’SS PWMSs (as might be expected since 5’SS and BPS are most important for determining exon-intron boundaries³³).

Length of the introns flanking exon 7. Because exons flanked by long introns tend to be skipped during the splicing process^{22–27}, we have examined whether E_7 is flanked by long introns. As observed in Fig. 3, I_6 varies dramatically in length between clades. The average length of I_6 is the largest amongst all introns for mammals ([2733,

Site	-5	-4	-3	-2	-1	1	2	3	4	5	6	7	8
A	0.2082	0.1306	0.3720	1.4204	-1.5830	-8.3696	-8.9985	1.0932	1.4771	-1.9859	-0.7113	0.0161	-0.5293
C	0.5104	0.6957	1.0657	-0.9485	-2.3528	-10.4401	-5.2125	-2.4697	-1.0419	-1.4937	0.0111	0.3350	0.6644
G	-0.7793	-0.4697	-0.9095	-1.4947	1.2021	1.4713	-9.4051	0.3050	-1.2529	1.1711	-0.6257	-0.0225	-0.3267
U	0.2021	-0.3378	-1.1008	-0.5682	-1.9475	-10.5499	2.2380	-3.5486	-1.0776	-1.8007	1.0212	-0.3701	0.2039
Species	5'SS ₆					PWMS ₆		5'SS ₇					PWMS ₇
Human	UCAAAGUAAGUGA					8.6625		AGGGG GUAAGAGC					5.0898
Chimpanzee	UCAAAGUAAGUCA					9.0200		AGGGG GUAAGAGC					5.0898
Mouse	UCAAAGUAAGUGA					9.5187		AGGGG GUAAGAAC					5.5747
Rat	UCAAAGUAAGUGA					9.3740		AGGGG GUAAGAAC					5.5747
Cow	UCAAAGUAAGUGA					9.1264		AGGGG GUAAGAGC					5.0898
Dog	UCAAAGUAAGUGA					9.1264		AGGGG GUAAGAGC					5.5361
Shrew	ACAAA GUAAGUGG					9.3351		CGGGG GUAAGCGC					6.5608
Armadillo	CCAAA GUAAGUCA					9.7922		AGGGG GUAAGAGC					5.5361
Opossum	UCCAA GUAAGUGA					9.9648		AGGGG GUAAGAGC					4.6637
Platypus	UCAAAGUAAGGGA					8.3157		CGGGG GUAAGAGC					4.8212
Chicken	GCAAA GUAAGAGU					5.6036		AGGGG GUAAGAGC					5.9924
Zebrafish	UCAAAGUAUGUCC					7.9026		AACAG GUCAGCUU					8.1978
Turtle	ACAAA GUAAGCAU					10.6407		GGGGG GUAAGACC					3.8889
Frog	ACAAA GUGAGUAU					8.5266		AAAGG GUAACUAU					6.4370

Table 1. The upper panel provides position weight matrix (PWM) for 15770 exon-intron junctions (5'SS) from human chromosome 22. The consensus sequence (CAGjGUAAGU) is shown in bold. The five exonic nucleotides are labeled as -5 to -1 and the 8 intronic nucleotides as 1 to 8. The lower panel gives position weight matrix scores (PWMS₆ and PWMS₇, respectively) for the 5' splice sites of introns 6 and 7 (5'SS₆ and 5'SS₇ in Fig. 1A(i)) from 14 vertebrate species according to the scoring matrix in the upper panel.

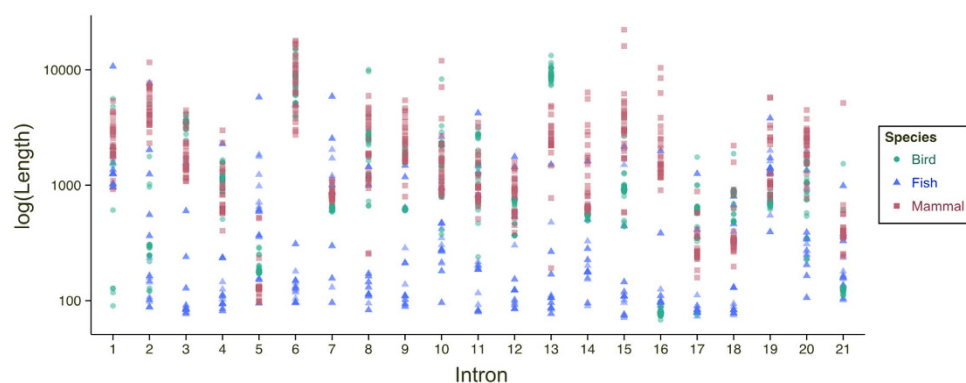


Figure 3. Length of USP4 introns for 62 bird, fish and mammal species. log₁₀ scale used for y-axis. Intron 6 is highly variable in length.

17911 nt) and second largest for birds ([3903, 15190] nt; second to I₁₃). Whereas I₆ is also relatively long in cartilaginous fish, the earliest-diverging clade presenting USP4 (shark = 4961 nt), it is contrastingly short in bony fish ([96, 310] nt). Altogether this suggests a large number of indels during the evolution of different vertebrate lineages, likely the most amongst all introns of USP4. Although exons with long flanking introns tend to be lost in the final mRNA^{22–27}, there is discrepancy concerning the relative effect of upstream and downstream introns. The detailed experimental study on CD44²² shows that exon skipping occurs only when the exon is flanked on both sides by long introns, and that the effect of the two introns appears to be symmetrical. However, subsequent studies on the relationship between intron length and exon skipping^{23,24} are not always consistent with these earlier findings. In particular, it appears as though the upstream intron has a greater effect on exon skipping than the downstream intron²⁵, which would suggest that the potential contribution of the long I₆ to E₇ skipping in mammals should not be ignored.

Experimental tests of alternative hypotheses. *Determination of splicing mechanism.* Although our results are consistent with the hypothesis that E₇ skipping results from BPS₇ strengthening relative to BPS₆ and 5'SS₆ stronger than 5'SS₇, they do not exclude the possibility that the longer intron I₆ or other potentially

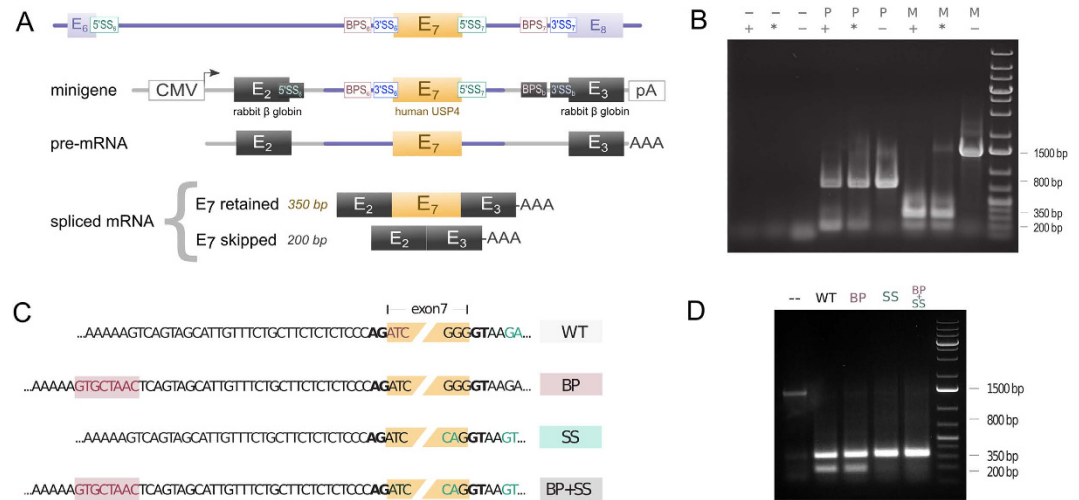


Figure 4. Mismatched flanking 5' splice site strengths leads to alternative skipping of exon 7. (A) Schematic of the RT-PCR assay construct. Assays were performed using oligonucleotide primers positioned upstream and downstream of the rabbit exons. (B) Exon skipping as detected in minigene RT-PCR assay. Lane labels specify transfected construct and reagents in U2OS cells. First line: –: untransfected control, P: empty plasmid (pXJ41), M: USP4-E7 minigene construct (pDG467). Second line: +: oligo dT-primed cDNA reaction, *: random-primed cDNA reaction, –: random primers, no reverse transcriptase (RT). A 200 base pair (bp) product of is visible after primed reactions of pXJ41-transfected cells. Exon-retained and -skipped products are visible as 350 and 200 bp bands, respectively, in pDG467-transfected cells. Products of approximately 800 and 1500 bp were generated pXJ41- and pDG467-transfected conditions, respectively, in the absence of RT and likely arose from amplification of DNA rather than cDNA. (C) Schematic of site-directed mutations. The wild type (WT) sequences and the boundaries of E₇ (yellow box) are shown. In the branch point (BP) mutant a YURAY sequence (indicated in pink) was inserted 32 residues upstream of E₇. In the splice site (SS) mutants the downstream exon-intron boundary sequence were optimized (substituted residues indicated in green). The combination mutant (BP + SS) incorporated both mutations. (D) RT-PCR analysis of site-directed mutants. Lane labels correspond to transfected mutant constructs as per Figure 4C. Exon-skipped products are absent from SS and BP + SS mutants.

complicating factors in USP4 pre-mRNA may contribute to E₇ skipping. To test the hypothesis that E₇ skipping is due to differential splice signals at 5' SS and BPS, we created a minigene construct by inserting the human USP4 genomic sequence encompassing E₇ (together with 75 nt at the 3' tail of I₆ and 51 nt at the 5' end of I₇) into the well characterized splicing reporter pXJ41 (the generous gift of Dr. Sushma Grellesheid, Durham University). In the resulting minigene the human E₇ genomic fragment resides in the second intron of the rabbit beta hemoglobin gene (Fig. 4A). If E₇ skipping is due to the long upstream I₆, then we should observe no E₇ skipping in this construct with short upstream intron. The minigene mimics the scenario in Fig. 1A(i) with the differential signal strength of splice sites: 5' SS_a (Fig. 4A) is stronger (PWMS = 7.5358) than 5' SS₇ (PWMS = 5.0898) and BPS₆ (Fig. 4A) is stronger than BPS₆, with the former having a CUAAC (YURAY) sequence located 35 nt from the 3' end of the intron and the latter having no YURAY at D_{to3',opt}. If E₇ skipping in its natural USP4 mRNA is due to such differential strength of splice signals, then we should observe E₇ skipping in the minigene mRNA.

When the minigene was expressed in human U2OS osteosarcoma cells, RT-PCR analysis using primers upstream and downstream of the rabbit exons revealed two isoforms of the size predicted for retention and exclusion of E₇ (Fig. 4B). Similar results were obtained in the unrelated HeLa cell line (not shown). This finding excludes exon skipping as a consequence of intron length but is consistent with E₇ skipping due to the differential strength of splice signals. We therefore explored the contributions of the BPS₆ and 5' SS₇ elements by site-directed mutagenesis of the E₇ minigene construct, inserting a consensus YURAY sequence at D_{to3',opt} in I_a (upstream of E₇) and/or engineering an optimized 5' SS₇ element in I_b (depicted as BP and SS respectively in Fig. 4C). The mutated versions of the minigene were transfected into U2OS cells and RT-PCR analysis was performed as before. Whereas the introduction of the consensus YURAY sequence had no effect on the ratio of exon retained and exon excluded products, the latter was undetectable in RNA isolated from cells transfected with minigenes in which the 5' SS₇ element had been optimized (Fig. 4D).

Phylogenetic distribution of USP4 alternative splicing. In contrast to mammalian species, 5' SS₆s of chicken and zebrafish USP4 are weaker than 5' SS₇s, as indicated by their PWMS values (Table 1). To verify whether (as would be predicted) E₇ skipping does not occur in such species, RT-PCR analysis was performed on RNA isolated from primary chick fibroblast cultures (the generous gift of Dr. J. S Diallo, Ottawa Hospital Research Institute). Primers corresponding to sequences in exons 6 and 8 were used to detect the presence or absence of the seventh exon as depicted in Fig. 5A. We detected only the exon-retained version of the transcript (Fig. 5B). However, when the human minigene was introduced into chick embryo fibroblasts by transfection both isoforms were detected (Fig. 5C). The absence of exon skipping in the chicken cells could thus be directly attributed to the primary

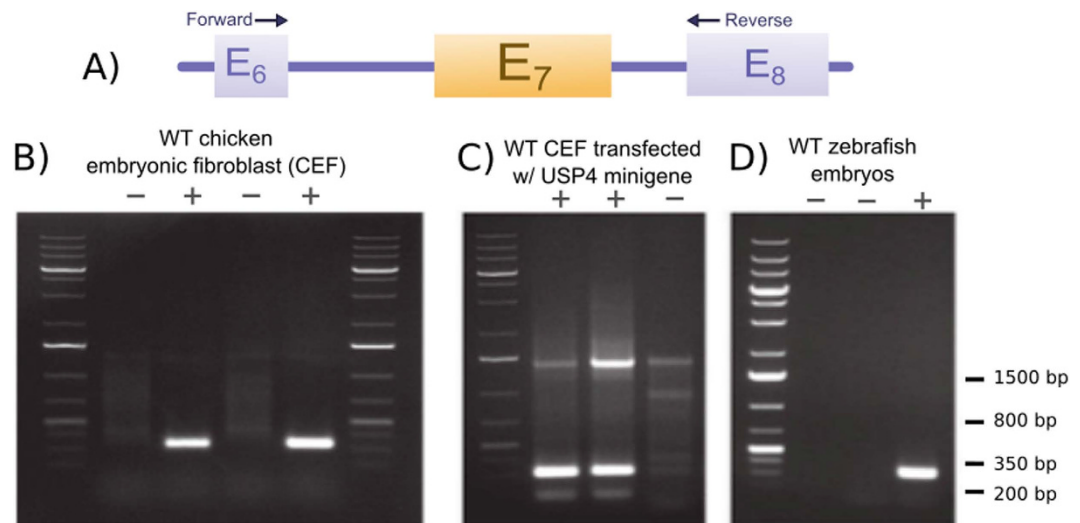


Figure 5. Exon skipping does not occur in the USP4 gene of the chicken or the zebrafish. (A) Schematic of the RT-PCR strategy using primers specific for exons 6 and 8. (B) RT-PCR analysis of RNA from the endogenous USP4 gene in chicken. Lane labels specify addition (+) or omission (–) of RT (control) to chicken embryonic fibroblast (CEF) RNA extracts. When RT was included a single PCR product of predicted size (329 bp) for the exon-retained transcript was detected. (C) RT-PCR analysis of CEF transfected with the human USP4 minigene construct. Lane labels specify transfection of pDG467 (+) or an irrelevant control plasmid (–) in CEF cells. Both the exon-retained and exon-included products were detected (as in human cells). (D) RT-PCR analysis of RNA from the endogenous USP4 gene in the zebrafish. Lane labels specify addition (+) or omission (–) of template (lane 2) or RT (lane 3) to larval zebrafish RNA extracts. A single amplification product was detected of the size predicted for the exon-retained cDNA (313 bp).

sequence of the chicken USP4 pre-mRNA. Our data exclude the possibility that E₇ retention occurs in the chicken as a consequence of an altered repertoire of splicing factors in avian versus mammalian cells (see Discussion). By similar logic we predict that exon skipping would not occur in the zebrafish gene; RT-PCR analysis of RNA from larval stage zebrafish (the generous gift of Dr. Marc Ekker, University of Ottawa) confirmed the presence of a single exon-retained isoform (Fig. 5D). In support of this, performing a BLASTn of USP4 exons 5–13 against the 600,432 chicken EST sequences recovered four sequences with E₇ but no sequence without E₇. Among the 1,488,339 zebrafish ESTs, seven have E₇ but none are without E₇. In contrast, searching the 8,704,868 human ESTs recovered five sequences with and seven without E₇. The corresponding numbers from the 4,853,570 mouse EST sequences are 20 and 8, respectively. Our conceptual framework based on the relative strengths of 5' splice signals thus correctly predicted splicing propensity in these model organisms, confirmed by both database and experimental analyses.

As is shown in Fig. 4D, the optimization of three nucleotides in the 5' splice site downstream of USP4-E₇ according to the consensus sequence, namely –3G → C, –2G → A and +6A → T, proved sufficient to eliminate exon skipping in the human USP4 minigene. Among species observed in Table 1, the nine therian mammal 5'SS₆s feature optimal nucleotides –2A and +6T while suboptimal –3G, –2G and +6A penalize the 5'SS₆ PWMs of all members of this lineage. These residues are identical in the Chinese turtle and are likely thus responsible for the observed alternative E₇ skipping in this distant relative. In contrast, both flanking splice sites of E₇ in zebrafish feature optimal nucleotides (5'SS₆: –3A, –2A, +6T; 5'SS₇: –3C, –2A, +6C), which preclude E₇ exclusion. Curiously, in chicken, these determinant nucleotides are identical to those of mammals which produce E₇ skipping with the exception of the 5'SS₆ +6N site, which is weak (+6A). The upstream and downstream 5'SSs in chicken, though weak, are equivalent and prevent exon skipping as in zebrafish. The +6N site may thus be the discriminant factor in E₇ skipping propensity. To verify this, we expanded the scope of our analysis to include all sequenced genomes bearing USP4 to see whether the 5'SS mismatching (in particular +6 site mismatching) predicts splicing proclivity. While direct expansion of our analytical framework is limited by insufficient EST data and biological sample unavailability, we can infer splicing patterns from RNA-seq datasets. Similar to the methodology used for EST mining, we performed a BLASTn of available RNA-seq data from the Sequence Read Archive (SRA) using the USP4 coding sequence with E₇ removed as a query. In the absence of hits crossing the exon 6–8 boundary for multiple, sufficiently large expression datasets, species were deemed to forgo short isoform production.

Figure 6A summarizes USP4 splicing patterns in a phylogenetic context with corresponding flanking 5'SS sequence logos indicated. According to the PWM in Table 1A, +6A and +6G weaken the 5'SS while +6T is optimal and +6C is neutral (weighted consensus illustrated in Fig. 6C). For all tetrapods, when the downstream +6 site is stronger than the upstream +6 site, there is alternative splicing of E₇. This correlation is particularly apparent in the avian phylum: chicken and turkey have no E₇ skipping (+6A; +6A), all other birds either exhibit skipping (+6C/T; +6A) or loss of E₇. What is more, some members of sister taxa have lost the ability to produce

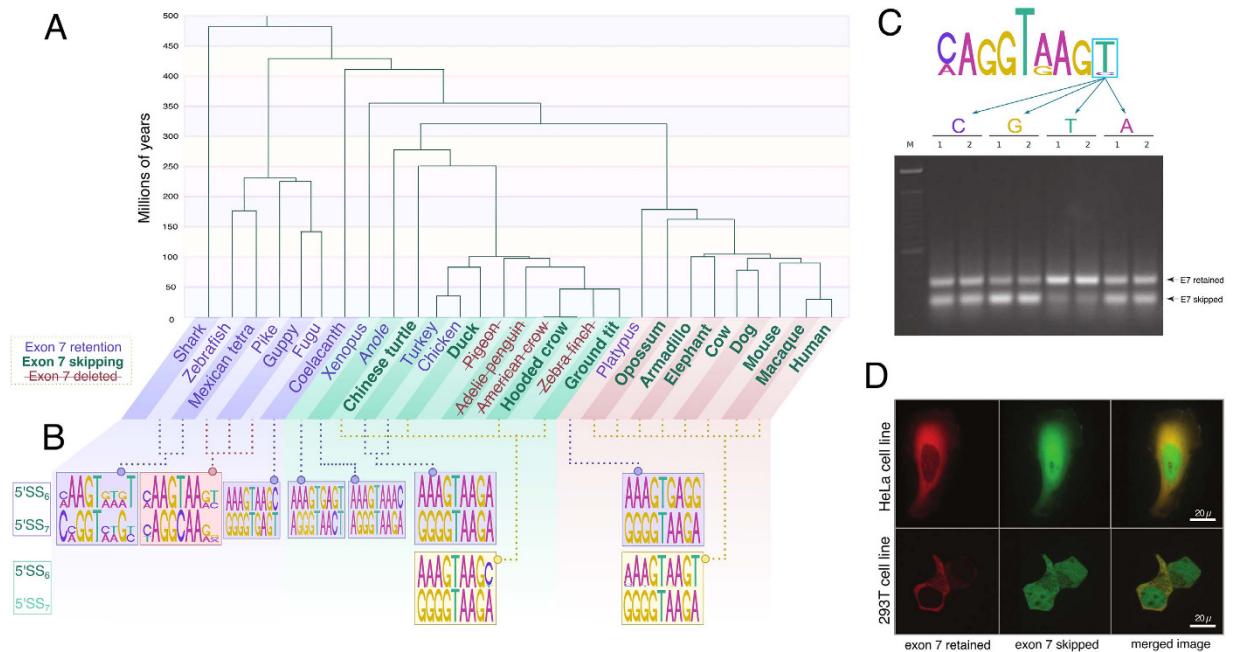


Figure 6. Long and short isoform production was selected for in therian mammals. (A) USP4 exon 7 skipping propensity throughout the vertebrate phylogeny (see inset Legend). (B) 5'SS₆ and 5'SS₇ identities for species in (A). In (B), splice site configurations that lead to constitutive retention of E₇ are in the top row and those that lead to alternative skipping are in the bottom row. (C) Sequence logo for an optimal 5'SS (from Table 1) and changes in long-to-short isoform ratios (IRL/S) after experimental replacement of the sixth intronic nucleotide (+6 site) of the downstream 5'SS₇ of human USP4 in H1299 cells. IRL/S quantifications are as follows: C = 1.00, G = 0.81, T = 1.52, A (WT) = 1.02. (D) Subcellular localization of exon 7 skipped and exon 7 retained USP4 isoforms. Long and short isoforms with appended green (GFP) and red (mKATE) fluorescent tags, respectively, were transfected into 293T and HeLa cells.

the long isoform: E₇ is deleted in *Corvus brachyrhynchos* but present in *Corvus cornix cornix*; absent from Adelle penguin but present in Emperor penguin, for example. In contrast to this substantial variability, all mammals retain an optimal E₇ skipping configuration, +6T; +6A (with the exception of the clade root: platypus USP4 has +6G; +6A and, consistent with our model, does not undergo skipping). In theory, many nucleotides substitutions could disrupt the 5'SS if alternative splicing were the result of drift. Since the same splice site configuration is maintained throughout 220 million years of mammalian evolution there may be selection for this particular +6 configuration. In Fig. 6C and Supplemental Figure 1, we show the effects of downstream +6 site point mutation from native +6A to +6T, +6C and +6G in human and mouse cell lines. In each case, the splicing propensity changed in direct relation with the estimated fitness in our PWM: alternative splicing was nearly eliminated in +6T, slightly reduced in +6C and increased in +6G. Therefore, we propose that the highly conserved +6A site within 5'SS₇ is under natural selection to maintain both long and short USP4 isoforms in therian mammals.

Differential localizations and roles of spliced isoforms. The evidence supporting alternative splicing selection in mammalian USP4 is strong; we would consequently expect the two isoforms to have distinct cellular roles. Indeed, we observed distinct subcellular localizations of long and short USP4 isoforms in both single- and double-transfections of HeLa, U2OS, 293T and 3T3 cells (see Fig. 6D). While the short isoform was distributed throughout the cell, the localization of the long isoform was largely cytoplasmic in most if not all cells in the four cell lines examined. Potential implications of this observation are discussed below. Altogether, our results suggest that the two major USP4 isoforms generated by alternative skipping of its seventh exon may not be functionally redundant as previously suggested.

Discussion

It has been proposed that mutations that weaken the 5' splice site are responsible for the evolutionary shift from constitutive to alternative splicing in many vertebrate genes, as reviewed in Keren *et al.*²¹, and compelling evidence has been presented in support of this hypothesis³⁴. While most minor splice variants are attributable to noisy splicing^{35,36}, USP4 constitutes a rare case wherein selective pressure acts to conserve differential 5'SS strengths leading to exon skipping in therian mammals. The approach we presented here focuses on these cis-acting splice sites, which offers a more basic but more direct framework towards understanding the splicing code. 5' splice sites can recruit trans-acting alternative splicing factors for intrinsic splice regulation. For example, deleterious exon skipping in survival of motor neuron (SMN) pre-mRNA can be attributed to recruitment of splice repressor U2AF65 by a weak downstream 5'SS³⁷. While trans-acting factors interacting with the 5'SSs of USP4 may similarly regulate E₇ skipping, our model explains USP4-E₇ splicing propensity independent of other cis-regulatory

sequences such as exonic splice enhancers (ESEs), which may or may not be selectively co-optimized in USP4 alternative splicing. Our study also highlights the importance of experimental verification of alternative hypotheses. Although the bioinformatics framework alone cannot distinguish between the two mechanisms proposed in Fig. 1(i,ii), the experimental results demonstrate that relative 5' SS strengths are far better predictors of alternative splicing than BPSs or upstream intron lengths. Further, our combinatorial *in silico* and experimental approach identified the +6 site within the 5' SS as the splicing discriminant. Intronic +6 site mutations have been reported as splicing instigators in other genes such as SMN1^{38,39}. E₇ skipping in SMN1 leads to spinal muscular atrophy (SMA), and SNPs that cause this aberrant skipping have been identified in patients at the downstream 5' SS₇ at the +6 site (+6T → G). SMN1 has a very close paralog, SMN2, that is incapable of rescuing SMN1 deficiency in SMA because its E₇ is also skipped due to a WT nucleotide variant, 5' SS₇ +6G. Thus, +6T at the downstream 5' SS₇ of SMN1/2 promotes upstream exon inclusion while +6G promotes near-total upstream exon skipping. In mammalian WT USP4, 5' SS₆ has +6T while 5' SS₇ has +6A. As reflected in the PWM in Table 1 and observed in Fig. 6C, the strengths of +6 site nucleotides are predicted to be as follows: T > C ≥ A > G, where a stronger 5' SS₆ +6 relative to 5' SS₇ +6 correlates with splicing proclivity. It is curious that +6A ≠ +6G and that the former was selected as the weak downstream nucleotide of USP4. A plausible mechanism for +6A-dependent alternative skipping may involve U1C, a component of the U1 snRNP that preferentially recognizes a 5' SS motif with +6A, GTATAA⁴⁰, and can interact with splicing regulator TIA-1^{41,42} to promote exon retention, for example in SMN2^{43,44}. Several genes undergo U1C-dependent alternative splicing^{45,46}. Based on linear changes in the relative abundances of the short and long isoforms observed during differentiation of P19 embryonic carcinoma cells (Gray, unpublished) we postulate that E₇ of USP4 may be subject to regulated alternative splicing in therian mammals.

Retention or exclusion of the amino acids encoded by exon 7 does not affect the protease activity of the USP4 enzyme (using a synthetic substrate¹⁴) and the ubiquitin-exchange regulatory mechanism proceeds equally in both USP4 isoforms¹⁶. We have nonetheless shown that there is selection for alternative splicing maintenance in mammalian USP4. Establishing the molecular selection driver should be highly informative. We show that the two isoforms display distinct subcellular localizations, which suggests that (1) propensity and/or (2) capacity for substrate interactions may differ. First, vital cytoplasmic (e.g. TGF-β pathway¹) and nuclear (e.g. spliceosomal^{11,12}) substrates have been reported for USP4 (isoforms specificities not declared). Long and short USP4 isoform production may be advantageous for simultaneous, collective targeting of key substrates in various cellular compartments. On the other hand, the two isoforms almost certainly have some distinct interactors. Cytoplasmic retention of USP4-long is mediated by phosphorylation of a ubiquitously conserved serine (S445); the apparent absence of this regulation in USP4-short may reflect a lack of phosphorylation by Akt². Exon 7 of mammalian USP4 is serine-rich (16 out of 47 residues; human sequence: RSSTAPSRNFTTSPKSSASPYSSVSASLIANGDSTSTCGMHSSGVSRG) and also contains six constitutively charged residues (five positively charged and one negatively charged). While the +4 net charge difference between isoforms likely affects substrate interactions, the serine-rich exon also retains multiple phosphorylation sites (underlined) that are conserved among all mammals. USP4-E₇ may be phosphorylated in conjunction with Ser445 for nuclear exclusion or may be required for interaction with Akt and other substrates. For instance, SART3, a spliceosomal factor and deubiquitination target of both USP4¹² and its paralog USP15⁴⁷, has been reported to interact with serine-rich (not to be confused with serine/arginine-rich) domains of proteins⁴⁸. Interestingly, USP15 contains an analogous, serine-enriched alternatively spliced seventh exon (SPGASNFSTLPKISPSSLSNNYNNMNNR; reported phosphorylation sites underlined). Splice boundaries and amino acid sequence differ between E₇ of USP4 and USP15, suggesting that alternative splicing arose independently in these, though they both maintain significant proportions of serines. This may be a case of stabilizing selection acting on clusters of phosphorylation sites⁴⁹. There may be an important feedback loop involving the splicing and subsequent localization of USP4 and USP15, two DUBs that critically interact with the spliceosome. Long and short USP4 production and thus DUB modification of isoform-specific substrates may differ across tissue types. It remains to be seen whether such isoform-specific substrates drove evolutionary conservation of the dual isoforms within placental mammals.

To summarize, we have shown that the long and short isoforms of USP4 have distinct properties and their contributions to cellular networks should be considered separately. Most proteins have more than one reported isoform, and though most may be considered non-essential noise, distinct functional variants, such as in USP4, must not be grouped as one protein. The roles of all significantly expressed minor splice variants should be studied more carefully.

Methods

Bioinformatic analysis. Well-annotated USP4 sequences for 62 vertebrate species were downloaded from GenBank (See Supplementary Table S2) covering major vertebrate taxa. Coding sequences, exons, introns, and exon-intron junctions (5 nt on the exon side and 12 nt on the intron side) were extracted and analyzed by using DAMBE⁵⁰. Shannon entropy (H) is used as a measure of site-specific sequence variability over a sliding window in Fig. 1C.

$$H = - \sum_{n=1}^N p_i \log_2 p_i \quad (1)$$

N in Eq. (1) is the number of character states (N = 20 for protein), and p_i is the frequency of each amino acid. To identify the optimal distance (D_{103',opt}) of branchpoint sites (BPS), we searched for the presence of YURAY motifs without downstream non-3' SS AG dinucleotides in all 15770 introns in human chromosome 22 and compiled D_{103'} defined as the number of nucleotides from the beginning of YURAY (human) to the 3' end of the

intron. The range that contains the majority of $D_{to3'opt}$ values is labeled $D_{to3'opt}$. We applied the same approach for chicken and zebrafish introns. To identify whether USP4 is subject to alternative splicing in diverse species, BLAST searches were performed using putative species-specific short isoforms (i.e., with exon 7 deleted) as a query against RNA-seq datasets from the Sequence Read Archive (SRA). RNA-Seq dataset identifiers are listed in the Supplementary Table S2.

RT-PCR analysis of spliced isoforms. The USP4 exon 7 reporter plasmid pDG467 was generated by insertion of a segment of human USP4 genomic DNA into the minigene reporter pXJ41. A segment of the USP4 gene on chromosome 3 (49348797–49349237) was amplified by polymerase chain reaction from H1299 cell DNA using Phusion high fidelity DNA polymerase (Thermo Scientific, Waltham, MA) with the forward primer AAAAAAGAATTCATTACAGGCACGAGCCACTG and the reverse primer AAAAAAGAATTCGCCCATCCCTTCATAAACAA (annealing temperature 55C). The resulting 699 base pair DNA product was digested with EcoRI and gel purified prior to ligation into the MfeI site of pXJ41. The branch point insertion plasmid pDG484 was generated using the Phusion site directed mutagenesis system (Thermo Scientific, Waltham, MA) with pDG467 as the template, forward primer 5'-GCTAACTCAGTAGCATTGTTTCTGCTTCTC-3', and reverse primer 5'-ACTTTTTGCAAAGAGCAAGCCCTATTTA-3' (68C annealing temperature). The splice donor optimization plasmid pDG485 was generated with pDG467 as the template, forward primer GTAAGTGCAGGTCCTTTCACCTGCTTC, and reverse primer CTGCTGCTGACACCGGAAGTGT (68C annealing temperature). The combination plasmid pDG468 was generated using the same primers and conditions, but using pDG484 as the template. Substitutions at the +6 position of the splice site were generated by polymerase chain reaction with pDG467 as the template. For all such substitutions the reverse primer CCCCTGCTGACACCGGAAGTGT was used. For the A to C substitution the forward primer was GTAAGCGCAGGTCCTTTCACCTGCTTC. For the A to G substitution the forward primer was GTAAGGGCAGGTCCTTTCACCTGCTTC. For the A to T substitution the forward primer was GTAAGTGCAGGTCCTTTCACCTGCTTC. The conditions for polymerase chain reaction were as above, but with an annealing temperature of 72C. The engineered mutations in all USP4-derived plasmids were verified before subsequent transfection experiments were performed. For analysis of splicing isoforms human U2OS cells, mouse NIH 3T3 cells or human H1299 cells (ATTC, Manassas, VA) were transfected at 50% confluence in 6 well dishes with 1 μ g of plasmid at 3 μ l of GeneJuice (EMD Millipore, Billerica, MA) using the manufacturer's protocol. RNA was harvested 24 hours post-transfection using a GeneJET RNA purification system (Thermo Scientific, Waltham, MA). Coupled reverse transcription/polymerase chain reaction was performed for each sample using the MyTaq One Step RT-PCR kit (BioLine, Taunton, MA) with forward primer GCTCCGGATCGATCCTGAGAAGT and reverse primer GCTGCAATAACAAGTTCTGC (60C annealing). RT-PCR products were analyzed on 1.2% agarose gels. DNA products were stained with Safe-Red (Applied Biological Materials, Inc., Richmond BC) and visualized using a UV gel camera apparatus (UVP, Upland CA).

Microscopy and imaging. To establish the localization of exon-retained and exon skipped isoforms of USP4, cDNAs corresponding to the mouse isoforms were obtained from Origene Technologies Inc. (Rockville, MD, USA) as C-terminal fusions with the red fluorescent protein mKATE or monomeric GFP, respectively. One microgram of each plasmid was introduced into cells cultured on cover slips using the GeneJuice transfection reaction (Millipore Canada, Etobicoke ON) following the supplied protocol. 24 hours post-transfection the cells were fixed for 10 minutes in 0.4% paraformaldehyde and were mounted in Vectashield mounting media (Vector Laboratories Canada, Burlington ON). Images were acquired using a Zeiss Axiovert 200M microscope equipped with the Apotome optical sectioning module.

References

- Aggarwal, K. & Massagué, J. Ubiquitin removal in the TGF- β pathway. *Nat Cell Biol.* **14**, 656–657 (2012).
- Zhang, L. *et al.* USP4 is regulated by AKT phosphorylation and directly deubiquitylates TGF- β type I receptor. *Nat Cell Biol.* **14**, 717–726 (2012).
- Fan, Y.-H. *et al.* USP4 targets TAK1 to downregulate TNF α -induced NF- κ B activation. *Cell Death Differ.* **18**, 1547–1560 (2011).
- Zhao, B., Schlesiger, C., Masucci, M. G. & Lindsten, K. The ubiquitin specific protease 4 (usp4) is a new player in the wnt signalling pathway. *J Cell Mol Med.* **13**, 1886–1895 (2009).
- Zhang, X., Berger, F. G., Yang, J. & Lu, X. USP4 inhibits p53 through deubiquitinating and stabilizing ARF-BP1. *EMBO J.* **30**, 2177–2189 (2011).
- Wang, L. *et al.* USP4 positively regulates RIG-I-mediated antiviral response through deubiquitination and stabilization of RIG-I. *J Virol.* **87**, 4507–4515 (2013).
- Xiao, N. *et al.* Ubiquitin-specific protease 4 (USP4) targets TRAF2 and TRAF6 for deubiquitination and inhibits TNF α -induced cancer cell migration. *Biochem J.* **441**, 979–986 (2012).
- Zhou, F. *et al.* Ubiquitin-specific protease 4 mitigates Toll-like/interleukin-1 receptor signaling and regulates innate immune activation. *J Biol Chem.* **287**, 11002–11010 (2012).
- Uras, I. Z., List, T. & Nijman, S. M. B. Ubiquitin-specific protease 4 inhibits mono-ubiquitination of the master growth factor signaling kinase PDK1. *PLoS One* **7**, e31003 (2012).
- Soboleva, T. A., Jans, D. A., Johnson-Saliba, M. & Baker, R. T. Nuclear-cytoplasmic shuttling of the oncogenic mouse UNP/USP4 deubiquitylating enzyme. *J Biol Chem.* **280**, 745–752 (2005).
- Sowa, M. E., Bennett, E. J., Gygi, S. P. & Harper, J. W. Defining the human deubiquitinating enzyme interaction landscape. *Cell.* **138**, 389–403 (2009).
- Song, E. J. *et al.* The Prp19 complex and the Usp4sart3 deubiquitinating enzyme control reversible ubiquitination at the spliceosome. *Genes Dev.* **24**, 1434–1447 (2010).
- Gupta, K., Chevrette, M. & Gray, D. A. The Unp proto-oncogene encodes a nuclear protein. *Oncogene.* **9**, 1729–1731 (1994).
- Frederick, A., Rolfe, M. & Chiu, M. I. The human UNP locus at 3p21.31 encodes two tissue-selective, cytoplasmic isoforms with deubiquitinating activity that have reduced expression in small cell lung carcinoma cell lines. *Oncogene.* **16**, 153–165 (1998).
- Gupta, K., Copeland, N. G., Gilbert, D. J., Jenkins, N. A. & Gray, D. A. Unp, a mouse gene related to the tre oncogene. *Oncogene.* **8**, 2307–2310 (1993).

16. Clerici, M., Luna-Vargas, M. P. A., Faesen, A. C. & Sixma, T. K. The DUSP-Ubl domain of USP4 enhances its catalytic efficiency by promoting ubiquitin exchange. *Nat Commun.* **5**, 5399 (2014).
17. Vlasschaert, C., Xia, X., Coulombe, J. & Gray, D. A. Evolution of the highly networked deubiquitinating enzymes USP4, USP15, and USP11. *BMC Evol Biol.* **15**, 230 (2015).
18. Alekseyenko, A. V., Kim, N. & Lee, C. J. Global analysis of exon creation versus loss and the role of alternative splicing in 17 vertebrate genomes. *RNA* **13**, 661–670 (2007).
19. Sugnet, C. W. *et al.* Unusual intron conservation near tissue-regulated exons found by splicing microarrays. *PLoS Comput Biol.* **2**, e4 (2006).
20. Sammeth, M., Foissac, S. & Guigó, R. A general definition and nomenclature for alternative splicing events. *PLoS Comput Biol.* **4**, e1000147 (2008).
21. Keren, H., Lev-Maor, G. & Ast, G. Alternative splicing and evolution: diversification, exon definition and function. *Nat Rev Genet.* **11**, 345–355 (2010).
22. Bell, M. V., Cowper, A. E., Lefranc, M. P., Bell, J. I. & Screaton, G. R. Influence of intron length on alternative splicing of CD44. *Mol Cell Biol.* **18**, 5930–5941 (1998).
23. Roy, M., Kim, N., Xing, Y. & Lee, C. The effect of intron length on exon creation ratios during the evolution of mammalian genomes. *RNA* **14**, 2261–2273 (2008).
24. Kandul, N. P. & Noor, M. A. F. Large introns in relation to alternative splicing and gene evolution: a case study of *Drosophila bruno-3*. *BMC Genet.* **10**, 67 (2009).
25. Fox-Walsh, K. L. *et al.* The architecture of pre-mRNAs affects mechanisms of splice-site pairing. *PNAS* **102**, 16176–16181 (2005).
26. Sterner, D. A., Carlo, T. & Berget, S. M. Architectural limits on split genes. *PNAS* **93**, 15081–15085 (1996).
27. Kim, E., Magen, A. & Ast, G. Different levels of alternative splicing among eukaryotes. *Nucleic Acids Res.* **35**, 125–131 (2007).
28. Patel, A. A. & Steitz, J. A. Splicing double: insights from the second spliceosome. *Nat Rev Mol Cell Biol.* **4**, 960–970 (2003).
29. Xing, Y. & Lee, C. Assessing the application of Ka/Ks ratio test to alternatively spliced exons. *Bioinformatics.* **21**, 3701–3703 (2005).
30. Gao, K., Masuda, A., Matsuura, T. & Ohno, K. Human branch point consensus sequence is yUnAy. *Nucleic Acids Res.* **36**, 2257–2267 (2008).
31. Zheng, C. L., Fu, X.-D. & Gribskov, M. Characteristics and regulatory elements defining constitutive splicing and different modes of alternative splicing in human and mouse. *RNA* **11**, 1777–1787 (2005).
32. Dewey, C. N., Rogozin, I. B. & Koonin, E. V. Compensatory relationship between splice sites and exonic splicing signals depending on the length of vertebrate introns. *BMC Genomics.* **7**, 311 (2006).
33. Matlin, A. J., Clark, F. & Smith, C. W. J. Understanding alternative splicing: towards a cellular code. *Nat Rev Mol Cell Biol.* **6**, 386–398 (2005).
34. Lev-Maor, G. *et al.* The “alternative” choice of constitutive exons throughout evolution. *PLoS Genet.* **3**, e203 (2007).
35. Melamud, E. & Moul, J. Stochastic noise in splicing machinery. *Nucleic Acids Res.* **37**, 4873–4886 (2009).
36. Pickrell, J. K., Pai, A. A., Gilad, Y. & Pritchard, J. K. Noisy Splicing Drives mRNA Isoform Diversity in Human Cells. *PLoS Genet.* **6**, e1001236 (2010).
37. Cho, S. *et al.* Splicing inhibition of U2af65 leads to alternative exon skipping. *PNAS* **112**, 9926–9931 (2015).
38. Wirth, B. *et al.* Quantitative Analysis of Survival Motor Neuron Copies: Identification of Subtle SMN1 Mutations in Patients with Spinal Muscular Atrophy, Genotype-Phenotype Correlation, and Implications for Genetic Counseling. *Am J Hum Genet.* **64**, 1340–1356 (1999).
39. Lorson, C. L., Hahnen, E., Androphy, E. J. & Wirth, B. A single nucleotide in the SMN gene regulates splicing and is responsible for spinal muscular atrophy. *PNAS* **96**, 6307–6311 (1999).
40. Du, H. & Rosbash, M. The U1 snRNP protein U1c recognizes the 5' splice site in the absence of base pairing. *Nature* **419**, 86–90 (2002).
41. Förch, P., Puig, O., Martínez, C., Séraphin, B. & Valcárcel, J. The splicing regulator TIA-1 interacts with U1-C to promote U1 snRNP recruitment to 5' splice sites. *EMBO J.* **21**, 6882–6892 (2002).
42. Bauer, W. J., Heath, J., Jenkins, J. L. & Kielkopf, C. L. Three RNA recognition motifs participate in RNA recognition and structural organization by the pro-apoptotic factor TIA-1. *J Mol Biol.* **415**, 727–740 (2012).
43. Singh, N. N. *et al.* TIA1 Prevents Skipping of a Critical Exon Associated with Spinal Muscular Atrophy. *Mol Cell Biol.* **31**, 935–954 (2011).
44. Klar, J. *et al.* Welander distal myopathy caused by an ancient founder mutation in TIA1 associated with perturbed splicing. *Hum Mutat.* **34**, 572–577 (2013).
45. Rösel, T. D. *et al.* RNA-Seq analysis in mutant zebrafish reveals role of U1c protein in alternative splicing regulation. *EMBO J.* **30**, 1965–1976 (2011).
46. Rösel-Hillgärtner, T. D. *et al.* A Novel Intra-U1 snRNP Cross-Regulation Mechanism: Alternative Splicing Switch Links U1c and U1-70k Expression. *PLoS Genet.* **9**, e1003856 (2013).
47. Long, L. *et al.* The U4/U6 recycling factor SART3 has histone chaperone activity and associates with USP15 to regulate H2b deubiquitination. *J Biol Chem.* **289**, 8916–8930 (2014).
48. Harada, K., Yamada, A., Yang, D., Itoh, K. & Shichijo, S. Binding of a SART3 tumor-rejection antigen to a pre-mRNA splicing factor RNPS1: A possible regulation of splicing by a complex formation. *Int J Cancer.* **93**, 623–628 (2001).
49. Landry, C. R., Freschi, L., Zarin, T. & Moses, A. M. Turnover of protein phosphorylation evolving under stabilizing selection. *Front Genet.* **5** (2014).
50. Xia, X. DAMBE5: A Comprehensive Software Package for Data Analysis in. *Mol Biol Evol.* **30**, 1720–1728 (2013).
51. Edgar, R. C. MUSCLE: multiple sequence alignment with high accuracy and high throughput. *Nucleic Acids Res.* **32**, 1792–1797 (2004).
52. Wickham, H. *ggplot2: elegant graphics for data analysis* (Springer New York, 2009).

Acknowledgements

This study was supported by Discovery Grants of the Natural Science and Engineering Research Council of Canada (NSERC) to X.X. and D.A.G. and by a grant from the Cancer Research Society, Inc. to D.A.G.

Author Contributions

C.V., X.X. and D.A.G. contributed equally to the design of the study and the preparation of the manuscript. C.V. and X.X. were responsible for computational analyses, while D.A.G. was responsible for the experimental aspects of the study.

Additional Information

Supplementary information accompanies this paper at <http://www.nature.com/srep>

Competing financial interests: The authors declare no competing financial interests.

How to cite this article: Vlasschaert, C. *et al.* Selection preserves Ubiquitin Specific Protease 4 alternative exon skipping in therian mammals. *Sci. Rep.* **6**, 20039; doi: 10.1038/srep20039 (2016).



This work is licensed under a Creative Commons Attribution 4.0 International License. The images or other third party material in this article are included in the article's Creative Commons license, unless indicated otherwise in the credit line; if the material is not included under the Creative Commons license, users will need to obtain permission from the license holder to reproduce the material. To view a copy of this license, visit <http://creativecommons.org/licenses/by/4.0/>